The Morphology of Equatorial Mg^+ Ion Distribution Deduced From 2800-Å Airglow Observations

J.-C. GÉRARD,[1,2] D. W. RUSCH,[1,3] P. B. HAYS,[1] AND C. L. FESEN[1]

The Visible Airglow Experiment on the Atmosphere Explorer E satellite has observed the resonantly scattered emission from Mg II at 2800 Å in the equatorial ionosphere. Altitude profiles of the Mg^+ ion distribution have been obtained from the inversion of the surface brightness measurements made on spinning orbits. These data show a daytime metallic ion layer between 150 and 200 km developing in the early morning and reaching about 100 ions/cm³ in the afternoon. Mg^+ ions are also seen in the F_2 region mostly in the late afternoon hours within a few degrees of the dip equator. The study of the vertical column density measured in the despun mode indicates that the amount of Mg^+ in the F region is most variable in the afternoon hours at low dip latitudes. These results can be explained in part by the diurnal variation of the $\mathbf{E} \times \mathbf{B}$ drift velocity which lifts the metallic ions up into the F region. The observations suggest that the vertical polarization electric field is not the primary transport mechanism extracting the Mg^+ ions from the low-altitude source layer.

INTRODUCTION

Magnesium and iron ions have been persistently observed with mass spectrometers in layers near 100 km at all latitudes. They are presumably produced by meteor ablation of metallic compounds followed by ionization or charge transfer from ambient NO^+ and O_2^+ ions. Their chemical lifetime is very long (>1 day), since they can only be removed by slow precesses such as radiative recombination or three-body reaction with O_2. In (the) recent years, various measurements have also found them in the F region, occasionally even above the F_2 peak. Their presence at high altitudes is attributed to upward transport by winds or electromagnetic drifts. Three major zones of metallic ions have been identified so far in the F region:

1. The first is a region associated with the daytime high-latitude polar cusp where Fe^+ ions have been measured by the Benett ion mass spectrometer on board the Atmosphere Explorer C satellite with density exceeding 30 ions/cm³ [*Grebowsky and Brinton,* 1978]. Mg^+ ions have also been detected optically in high-latitude evening twilight by *Gérard* [1976] using the Ogo 4 ultraviolet spectrometer. The lifting mechanism is probably the drift generated by the strong convection electric field existing in this region.

2. The second is a zone mapping the mid-latitude ion trough where winds blowing equatorward carry the ions along the field lines during daytime [*Grebowsky and Brinton,* 1978].

3. The third is the equatorial daytime and nighttime ionosphere where Fe^+ ions were observed by *Hanson and Sanatani* [1970] using a retarding potential analyzer on the Ogo 6 satellite. They found that Fe^+ could be detected above the F_2 peak near the dip equator in densities sometimes exceeding 1000 ions/cm³. Optical measuremtns of Mg^+ 2800-Å twilight airglow above 540 km were reported by *Gérard and Monfils* [1974] and *Gérard* [1976] within approximately 20° of the dip equator. A transport mechanism specific to the equatorial region has been proposed by *Hanson et al.* [1972]. It combines vertical motion of the metallic ions in the E region under the effect of the vertical polarization electric field associated with the equatorial electrojet with subsequent $\mathbf{E} \times \mathbf{B}$ vertical drift lifting up the ions during daytime.

The optical observations briefly described above were largely unplanned and had a limited local time and altitude coverage. One of the filters of the Visible Airglow Experiment on board the Atmosphere Explorer E satellite was centered to the resonance doublet of Mg II at 2800 Å. It has provided new results concerning the morphology of the Mg^+ ions in the equatorial ionosphere and its variations. This paper describes the observational technique and presents new data about the altitude, local time, and latitudinal distributions of Mg^+.

RESONANCE SCATTERING

The Mg II ^2S-^2P doublet at 2795.5–2802.7 Å is excited in the earth's atmosphere by resonance scattering of the solar ultraviolet radiation. The oscillator strength of the two lines are $f_{2795} = 0.627$ and $f_{2802} = 0.313$ [*Wiese et al.,* 1966]. The emission rate factors of the two components have been calculated by *Anderson and Barth* [1971] as $g_{2795} = 0.091$ and $g_{2802} = 0.037$ photon s^{-1}. If the atmosphere is optically thin for these lines, the column density is simply related to the column emission rate by the relationship

$$I = 1 \times 10^{-6} g \int [Mg^+]\, dl$$

where I is expressed in rayleighs and dl is the element along the line of sight. In the case of a broadband photometric measurement such as this one, g denotes the total emission rate factor of the doublet, equal to 0.13 photon s^{-1}.

If the column density exceeds a critical value, the transition becomes optically thick, and this simple relationship may not be applied. The resonance scattering cross section for a Doppler-broadened line of central frequency ν_0 is given by

$$\sigma_\nu = \frac{\pi e^2}{mc} f \frac{c}{\nu_0}\left(\frac{2\pi kT}{m}\right)^{-1/2} \exp\left[-\frac{mc^2}{2kT}\left(\frac{\nu-\nu_0}{\nu_0}\right)^2\right]$$

where m denotes the electron mass, m the atom mass, and the other symbols have their usual meaning. In the case of the 2795-Å line the cross section at the line center is 6.7×10^{-12} cm² for $T = 200$°K. Hence the ion column density required to reach $\tau = 1$ is 1.5×10^{11} cm^{-2}, which corresponds to a doublet intensity of 19 kR.

Anticipating the results described below, the overhead intensity never exceeds 300 R, and maximum horizontal in-

[1] Space Physics Research Laboratory, Department of Atmospheric and Oceanic Science, University of Michigan, Ann Arbor, Michigan 48109.

[2] Institut d'Astrophysique, Université de Liége, 4200 COINTE, Belgium.

[3] Now at Laboratory for Atmospheric and Space Physics, University of Colorado, Boulder, Colorado 80309.

Paper number 9A0617.
0148-0227/79/009A-0617$01.00

tensity in the E region is of the order of 8 kR. Consequently, these optical thickness effects can be neglected in converting the 2800-Å emission rates into column densities.

By contrast, in the twilight observations of a sporadic E layer by *Anderson and Barth* [1971], a vertical column density η_V of at least 4×10^9 ions/cm^2 was reported. Therefore the horizontal ion column density η_H along the grazing solar rays was approximately

$$\eta_H = \eta_V(\pi R/2H)^{1/2}$$

where R is the geocentric altitude and H is the topside scale height. Using $H = 1$ km, the horizontal column is 4×10^{11} cm^{-2}, and $\tau \simeq 2.7$ at the tangent point. This explains why the intensities of the two doublet lines were not in the ratio of the g factors.

Observational Technique

The visible airglow experiment (VAE) [*Hays et al.*, 1973] is a conventional filter photometer designed to monitor various airglow and auroral emission features. The VAE has two distinct optical channels, one with high sensitivity used where angular resolution is unimportant (3° half-angle cone) and a second less sensitive channel with a narrow (3/4° half-angle cone) field of view to provide good angular and spatial resolution. The observations reported here were made by the VAE on the AE-E spacecraft using a filter centered at 2800 Å with a 20-Å band pass to measure solar radiation resonantly scattered by Mg$^+$ ions. We have assumed that with the exception of the continuum emissions from Rayleigh scattering and the galaxy, only Mg$^+$ resonantly scattered emission is measured through the 2800-Å filter. The AE-E spacecraft is in an orbit inclined by 23° to the equator.

The high-sensitivity channel is used to map the overhead surface brightness to determine, in a statistical sense, local time and magnetic latitude variations of the Mg$^+$ column density. The overhead surface brightness is given by

$$I_{2800}(Z_{sat}) = 1 \times 10^{-6}\, g \int_{Z_{sat}}^{\infty} N_{Mg^+}(Z)\, dZ$$

where I is the intensity in rayleighs, g is the efficiency for resonance scattering described earlier, and $N_{Mg^+}(Z)$ is the Mg$^+$ density. We have compiled local time and magnetic latitude maps of Mg$^+$ vertical emission by sorting the data into altitude bins for both ascending and descending legs. The statistical accuracy of the data is increased, and the intensity is averaged over several degrees along the satellite path equal to a few minutes in local time. The results are described in the following section.

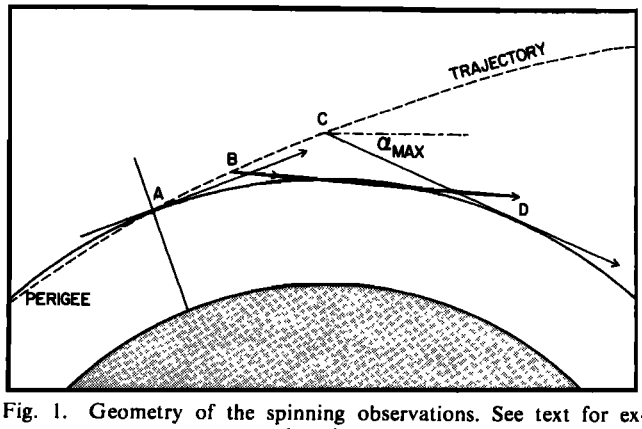

Fig. 1. Geometry of the spinning observations. See text for explanations.

The narrow channel of the VAE is primarily used to perform limb scanning experiments when the spacecraft is spinning. In Figure 1 we display the spatial geometry of the measurements. These data are used to derive local volume emission rates by the technique described by *Hays and Roble* [1972] and *Hays et al.* [1973]. This technique yields vertical profiles of the volume emission rate under the assumption of a spherically stratified atmosphere. In this experiment we have used, in each spin, data from six integration periods (0.032 s) above and below the horizontal direction for each inversion, corresponding to $\alpha_{max} = 4.6°$. The inverted data from each spin are then averaged to provide one profile. Normally, two average profiles are derived from each orbit, one for the downleg and one for the upleg. The use of six data points provides volume emission rates from the satellite altitude to approximately 25 km below the satellite. During a typical orbit, data will be averaged from about eight consecutive forward or backward limb scanning inversions (points A to C) to provide the volume emission rate at one altitude. The satellite moves approximately 1° along the orbit between limb scans and, in addition, must look farther forward along the orbit and deeper into the atmosphere to measure the same altitude in each succeeding spin. As a result, the data are averaged over about 15° from A to D, or, for the AE-E orbit, about 1 h in local time. Only data from the elliptical phase of AE-E were used for the limb scanning experiment.

All data for which the viewing direction of the sensitive channel was within 45 degrees of the sun were eliminated to avoid potential contamination by white light scattered off the baffling system. This accounts for the gap in the data near noon in the results described below. All data taken when AE-E was in the South Atlantic Anomaly above 200 km were eliminated. Galactic emissions also contaminate the sensitive channel measurements. This background was removed by examining data from high-altitude orbits.

Observations

The data. An example of the 2800-Å data is shown in Figure 2 for the despun elliptical orbit 1082. The vertical emission rate measured by the wide angle channel is plotted versus time and various other parameters of the orbit. The intensity shows large-scale variations from 7 to 300 R as well as small-scale structures. The number density of Mg$^+$ and Fe$^+$ ions detected by the Benett ion mass spectrometer (Bims) [*Brinton et al.*, 1973] on the same orbit is plotted for comparison. The sensitivity threshold of the mass spectrometer for these ions is approximately 20 ions/cm^3 on AE-E. There is clearly good correlation between the measurements of the two instruments, especially near the density peak. However, it must be borne in mind that the airglow intensities depend on the column density above the satellite, whereas the mass spectrometer gives the density along the trajectory. This difference, combined with the lower sensitivity of the Bims experiment, explains the absence of peak-to-peak correlation for the secondary maxima.

This comparison shows that measurements of resonantly scattered radiation at 2800 Å may be confidently used to study the morphology of metallic ions in the daytime ionosphere. This example also illustrates the complexity of the morphological study: the fact that the 2800-Å intensity does not monotonically increase with decreasing altitude indicates that other variables such as local time, latitude, and possibly longitude

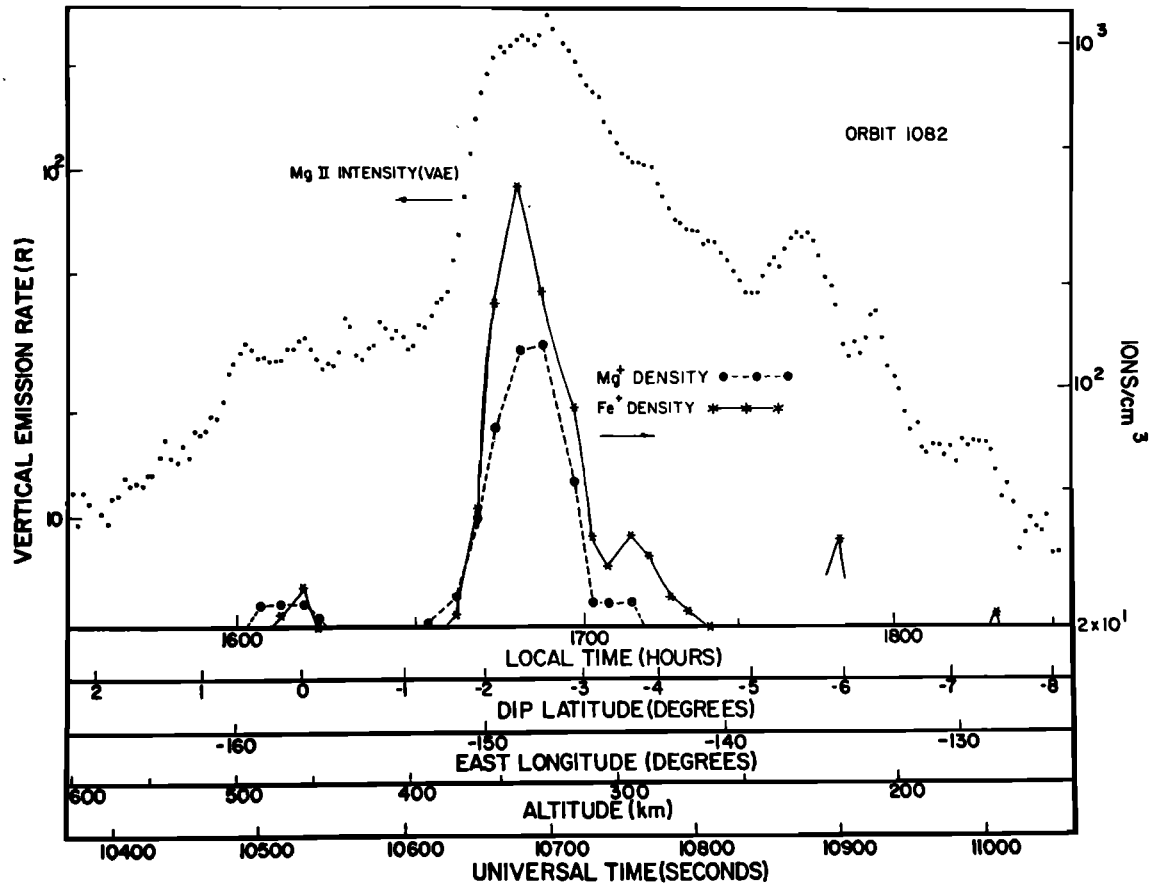

Fig. 2. Measurements of the 2800-Å vertical emission rate by VAE and Fe^+ and Mg^+ densities by Bims on downleg of orbit AE-E 1082.

also control the ion distribution in the F region. The study of these various effects is reported in subsequent sections.

Figures 3 and 4 show examples of data obtained in the spinning mode with the narrow angle channel. The orbit parameters for perigee are listed in Table 1. The count rate per integration period is plotted versus the altitude of the tangent point:

$$Z_t = (R_E + Z_s) \cos \theta - R_E$$

where R_E is the earth radius, Z_s the spacecraft altitude, and θ the angle of the line of sight with the horizontal direction. For this channel, 1 count/integration period corresponds to 43 R. Also shown for comparison is the contribution of the Rayleigh scattering in the filter band pass calculated using a model atmosphere. Below 105 km the measured intensities follow exactly the Rayleigh scattering curve. This is an independent check of the instrument sensitivity and indicates that no useful data on the Mg^+ ions may be obtained below about 120 km. On the other hand, above 140 km the Rayleigh scattering contribution becomes negligible, and no correction needs to be made to the measurements. There is a clear difference in the ion distribution between the morning (orbit 423) and the afternoon (orbit 792) profiles. An almost constant scale height of 75 km is deduced from the distribution on orbit 792.

Measurements of the vertical column density. The data gathered with the wide angle channel on despun orbits have been used mostly for a statistical study of the diurnal and latitudinal variation of the overhead vertical intensity. The diurnal variation of the vertical ion column density was obtained at different altitudes from the oriented observations of the elliptical phase of the AE-E mission. The period of time covered by these data extends from December 12, 1975, to February 26, 1976 (about 55 orbit legs).

Figure 5 shows these results for two altitude ranges centered at 180 km and perigee (≃145 km). The gap in the data near noon is due to the removal of the measurements contaminated by stray solar radiation in the instrument. The galactic back-

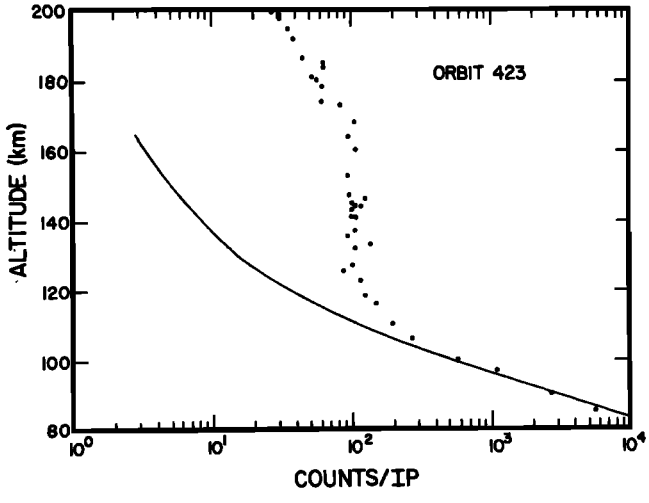

Fig. 3. Intensity of the 2800-Å signal measured on spinning orbit AE-E 423 versus the altitude of the tangent point. The solid line is the calculated Rayleigh scattering curve. Local time is 10.3 hours. Counts/IP is counts per integration period.

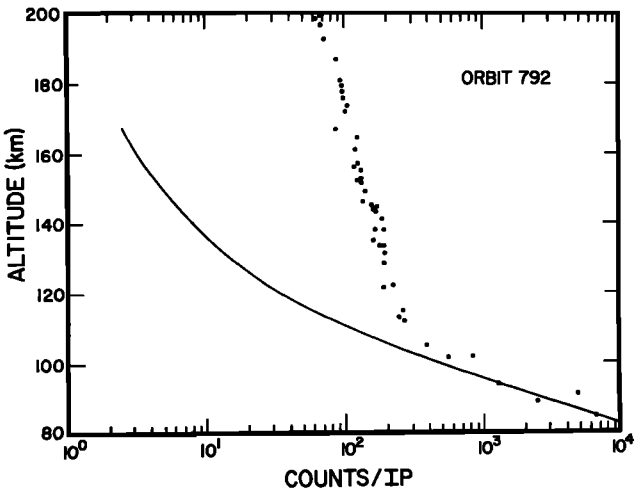

Fig. 4. Intensity of the 2800-Å signal measured on spinning orbit AE-E 792 versus the altitude of the tangent point. The solid line is the calculated Rayleigh scattering curve. Local time is 15.8 hours. Counts/IP is counts per integration period.

ground, data contaminated by planets and the South Atlantic Anomaly, has been removed.

The observations show a marked increase of the intensity from sunrise to 1000 LT at both altitudes. The intensity tends to decrease during the afternoon hours until local sunset (SS). The column density of ions is larger above 145 km than above 180 km, especially during morning hours, indicating that a major fraction of the Mg^+ is located below 180 km. The maximum brightness occurs in the gap between 1000 LT and 1400 LT and most probably near 1400 LT. The brightest intensities at perigee reach about 300 R, which implies a vertical column of 2×10^9 ions/cm^2. It is obvious that at both altitudes the scatter of intensity is much larger after noon than before noon and the scatter increases to nearly an order of magnitude at or after sunset. Thus the morning development of the *F* region layer is more regular and orderly than the subsequent transport later in the day. This point will also be demonstrated by the spinning data.

Results of the spinning mode. Observations made with the narrow angle channel on approximately 50 AE-E spinning elliptical orbits (orbits 246 to 1184) were inverted by using the Abel integral inversion. The period of time covered by these observations extends from December 19, 1975, to February 3, 1976. Consequently, little seasonal variations are expected in this short time interval.

Figure 6 shows a selection of 12 typical profiles of Mg^+ ions in the *F* region in the order of increasing local solar time. The parameters of the observations are given in Table 1 and refer to the location when observing at a tangent point of 150 km from an altitude of 170 km (cf. Figure 1). There is clearly an important diurnal variation in the shape and density of the layer. Starting after sunrise from a weak layer peaking below 150 km, the layer develops regularly throughout the morning. The peak moves up in altitude, reaches a maximum near 1400 LT, and collapses during the afternoon. This behavior is in agreement with the upward looking observations described before. The morning distribution is characterized by a well-defined layer peaking between 160 and 200 km. It is detected as early as 0620 LT at dip latitudes as high as 30°. The afternoon distribution is often characterized by a quasi-exponential decrease with a scale height of the order of 40 km. The late afternoon behavior is quite variable and may exhibit a high-altitude tail, as will be shown below. No evidence is found of a latitudinal dependence of the density and altitude of the peak in the morning hours. In contrast, the F_2 region tail observed at evening twilight is associated with small dip latitudes.

The variability of the altitude distribution is illustrated by Figure 7, where all the profiles obtained in three specific ranges of local times have been plotted together. The early morning data illustrate the features already mentioned, namely, a layer with a maximum density of about 20 ions/cm^3 with a well-defined peak. Some scatter in the profiles is due to the low count rate and to missing telemetry data for parts of the profiles, but the actual variability is in fact rather small. The early afternoon profiles show densities between 50 and 100 ions/cm^3 near 150 km and are all relatively similar. The late afternoon distribution is highly variable in shape and magnitude and may either drop below detectability below 200 km or extend as high as 500 km. It must also be remembered that the observational technique is such that the profiles obtained by this method are averaged over a fairly long interval of local time and longitude. Consequently, the inverted profiles do not

TABLE 1. Orbit Parameters for Data of Figures 3, 4, and 6

Orbit*	Date†	Local Time, hours	Solar Zenith Angle, deg	Geographic Latitude, deg‡	Geographic Longitude, deg§	Dip Latitude, deg‡
356	75352	6.6	88	16	130	8
252	75344	6.9	79	3	−86	14
348	75352	8.5	67	19	28	9
373, D	75354	9.0	61	20	33	10
373, U	75354	9.6	55	19	41	10
398	75356	10.0	49	17	45	8
423	75358	10.3	43	13	40	4
736	76018	12.9	16	−11	138	−20
766, D	76020	13.7	31	−2	19	−12
766, U	76020	15.0	51	5	37	−4
792	76022	15.8	65	13	60	5
864	76028	15.1	58	18	176	14
844	76026	16.2	73	19	37	10
943	76034	18.0	93	12	154	5

*D denotes a downleg; U, an upleg.
†Read 75352 as day number 352 of 1975.
‡Positive values refer to northern latitudes; negative values, to southern latitudes.
§Positive values refer to east longitudes; negative values, to west longitudes.

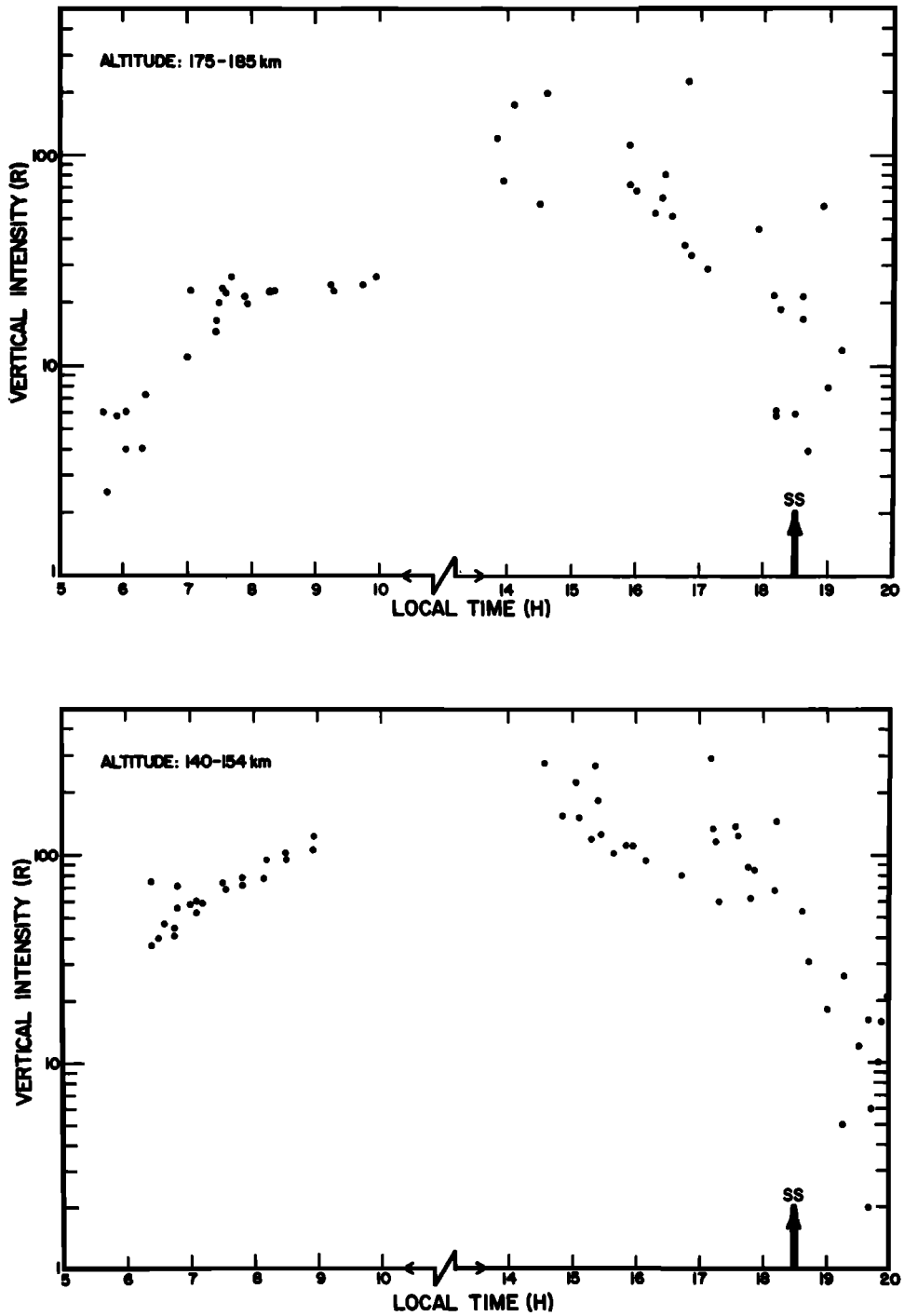

Fig. 5. Vertical emission rate of the Mg^+ airglow versus local solar time at two different altitudes. The arrows show the time of local sunset (SS). Note the break in the time axis near noon.

necessarily reflect the real vertical distribution at one location but are averaged along the satellite track. It is possible that at a given altitude a mass spectrometer would reveal highly structured regions which are not revealed by this method of analysis of the spinning observations.

The E region Mg^+ layer has been investigated following the method described previously. In Figure 8, spins of five orbits at different local times have been plotted versus the altitude of the tangent point. The orbit parameters for perigee are listed in Table 2. The data show that the diurnal variation in the E region is similar to that in the F region. For example, at 120 km a variation by a factor of 2.5 is observed between early morning and early afternoon intensities. Here again a peak is seen near 1400 LT, and the layer collapses during the afternoon. There is no indication of any magnetic latitude dependence in the profiles as may be seen in Figure 8 where the dip latitudes vary from 2° to 30°. As was discussed earlier, a unit optical depth is reached at the center of the 2795-Å line for a column density of 1.5×10^{11} cm^{-2}. At twilight the path of the solar radiation in the layer is maximum. The total path to take into account is twice the horizontal column density measured from the tangent point, which is equal to I_h/g, where I_h is the

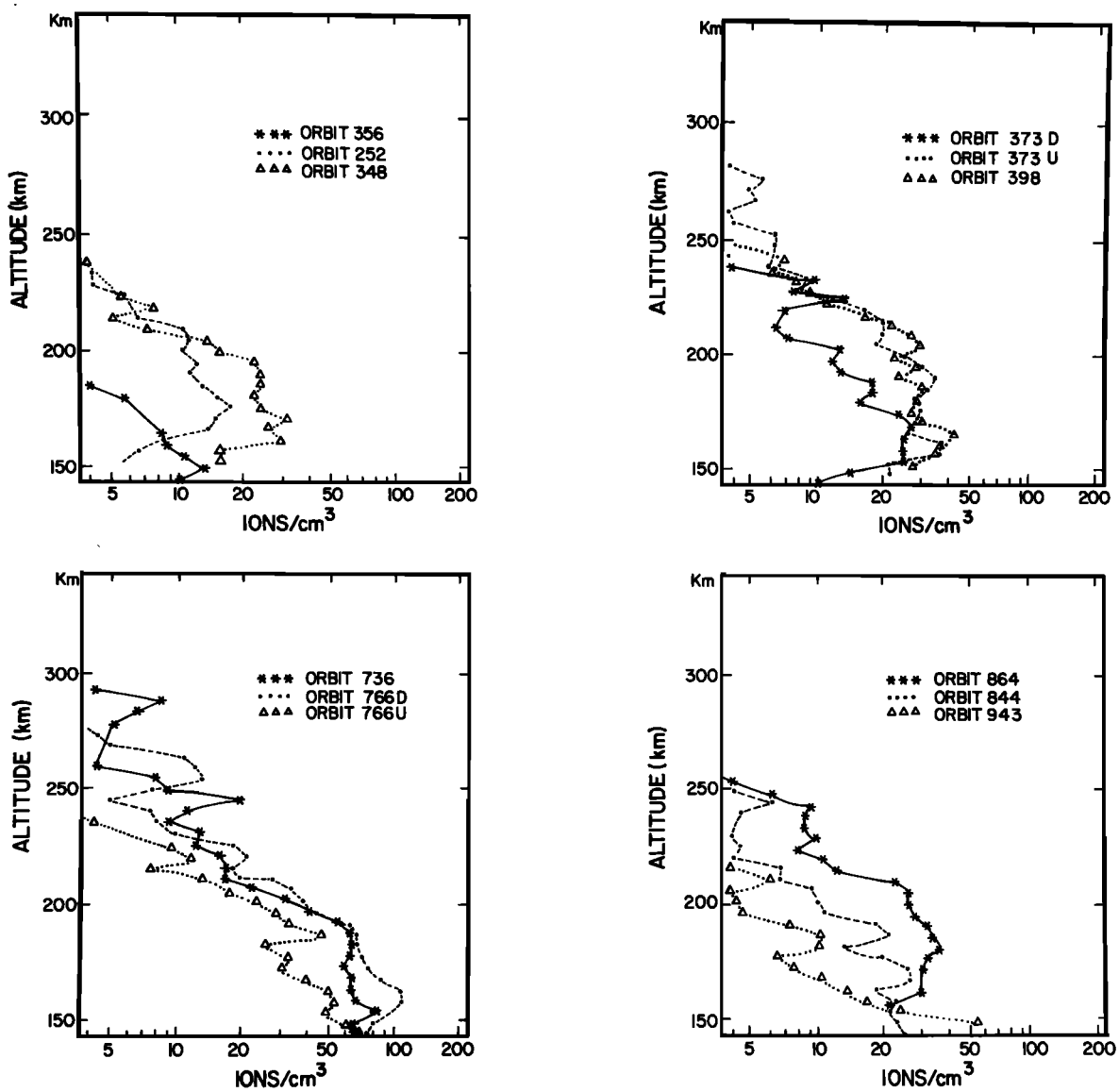

Fig. 6. A selection of Mg^+ density profiles obtained by Abel inversion of the 2800-Å airglow on spinning orbits. The local times are as follows; orbit 356, 6.6 hours; orbit 252, 6.9 hours; orbit 348, 8.5 hours; orbit 373D, 9.0 hours; orbit 373U, 9.6 hours; orbit 398, 10.0 hours; orbit 736, 12.9 hours; orbit 766D, 13.7 hours; orbit 776U, 15.0 hours; orbit 864, 15.1 hours; orbit 844, 16.2 hours; and orbit 943, 18.0 hours.

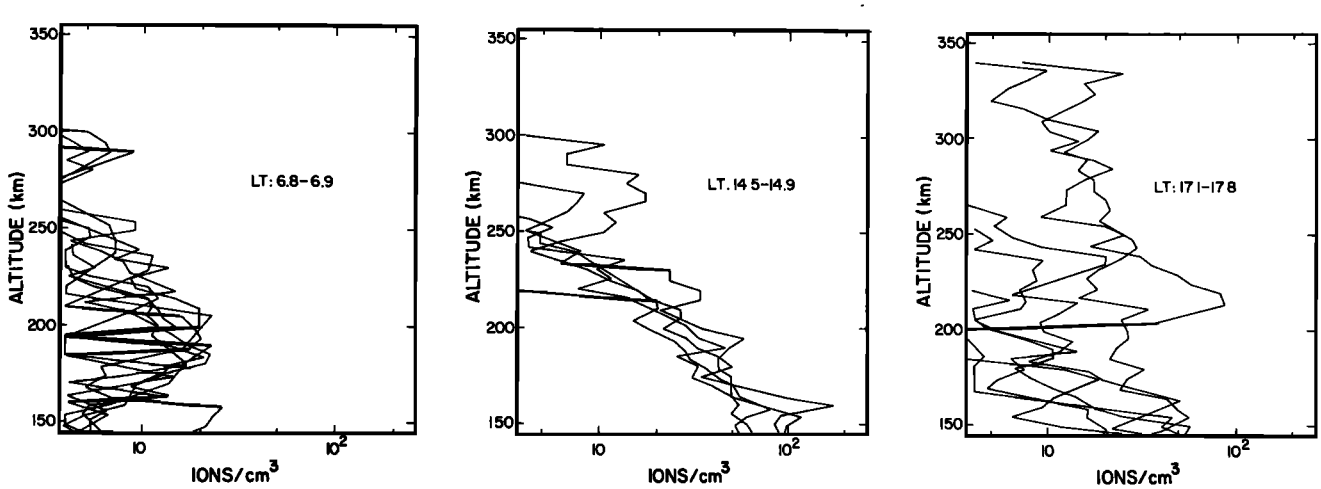

Fig. 7. Mg^+ density profiles observed at three different local times.

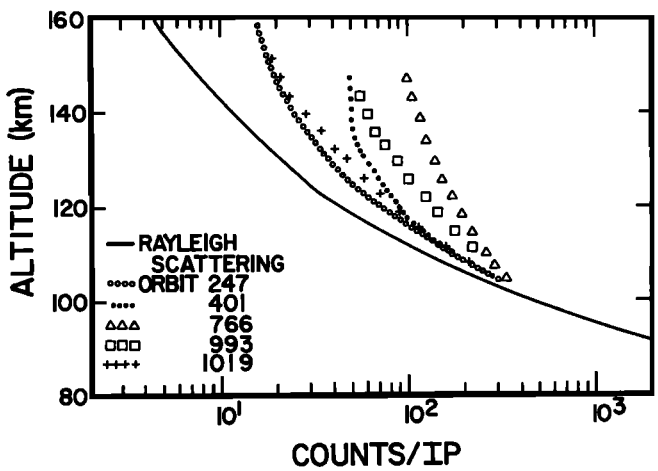

Fig. 8. Intensity of the 2800-Å airglow in the E region versus the altitude of the tangent point for five different orbits. The local times are as follows: orbit 247, 6.3 hours; orbit 401, 8.8 hours; orbit 766, 14.4 hours; orbit 993, 18.3 hours; and orbit 1019, 18.4 hours. The solid line is the calculated Rayleigh scattering contribution. Counts/IP is counts per integration period.

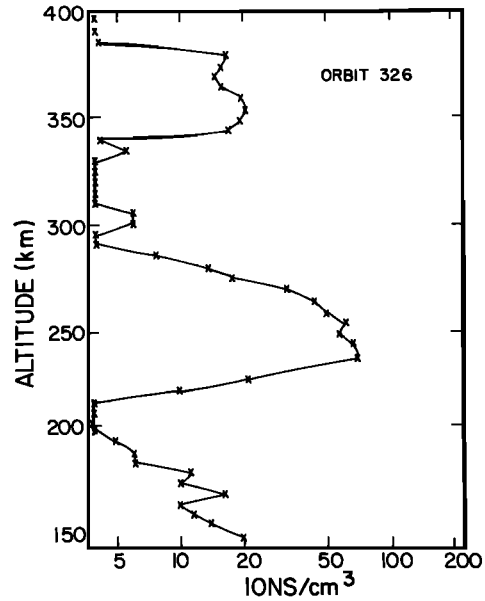

Fig. 9. Mg^+ density profile for orbit 326. The parameters of the observation are listed in Table 3.

emission rate plotted in Figure 8. Taking I_h = 8 kR, we deduce $\tau \simeq 0.4$. Since this value refers to the line center of the brightest of the doublet components, it is concluded that the optical thickness does not affect significantly the observations, even in the most unfavorable case.

Special features. The profiles illustrated in Figure 6 were selected as typical examples of the spinning data. Actually, some profiles show remarkable differences which may often be associated with the parameters of the observations. Figures 9 to 13 show a few profiles different from those of Figure 6. The orbital parameters are listed in Table 3.

Figure 9 presents the profile measured on orbit 326 at 0800 LT. This peculiar profile shows, in addition to the regular layer below 200 km, two F region peaks at 240 and 350 km. This feature is very unusual at this time of the day and is in fact a unique case. It is most probably the consequence of the high dip latitude of the observations (29°N). It is believed that such layers are formed of ions transported poleward from lower latitudes during previous daytime hours and maintained in the F region throughout the night by converging thermospheric winds having significant parallel field components at this latitude.

Orbit 743 shown in Figure 10 is an example of an afternoon profile exhibiting a quasi-constant density over a wide altitude range followed by a steep topside gradient. Topside scale heights as small as 7 km have been observed occasionally, in agreement with the independent measurements reported by *Gérard and Monfils* [1978]. These features have been observed on several occasions during the afternoon hours but do not show evidence of a latitude dependence. Figure 11 shows a midafternoon profile with a double peak at very low magnetic latitude. Such double layers are frequently observed in the afternoon and may be explained by irregular time variations in the **E** × **B** drift such as electric field reversals before sunset associated with the occurrence of counterelectrojets [*Woodman et al.*, 1977]. *Hanson et al.* [1972] have shown that the effect of such pertubations in the electric field is to cause multiple peaks in the vertical ion distribution.

Orbit 993 (Figure 12) shows the case of a low-latitude late afternoon profile exhibiting a long high-altitude tail. This type of profile is frequently observed within a few degrees of the dip equator at the end of the afternoon but is normally not seen at dip latitudes exceeding ~10°. These are layers of the type observed by the TD-1A satellite above 540 km at evening twilight and whose morphology has been described by *Gérard and Monfils* [1978]. However, the emission rates measured with the TD-1A instrument tended to be higher than those reported here. This may be an effect of the variation of the solar activity between 1972 and 1976.

The profile observed on orbit 1019 and displayed in Figure 13 is clearly composed of several curves corresponding to different spins or group of spins. This is most probably due to

TABLE 2. Orbit Parameters for Data of Figure 8

Orbit	Date*	Local Time	Solar Zenith Angle, deg	Geographic Latitude, deg†	Geographic Longitude, deg‡	Dip Latitude, deg†
247	75344	6.3	85	0	23	−10
401	75356	8.8	63	19	−59	30
766	76020	14.4	41	2	28	−8
993	76038	18.3	94	3	−164	3
1019	76040	18.4	96	−2	−168	−2

*Read 75344 as day number 344 of 1975.
†Positive values refer to northern latitudes; negative values, to southern latitudes.
‡Positive values refer to east longitudes; negative values, to west longitudes.

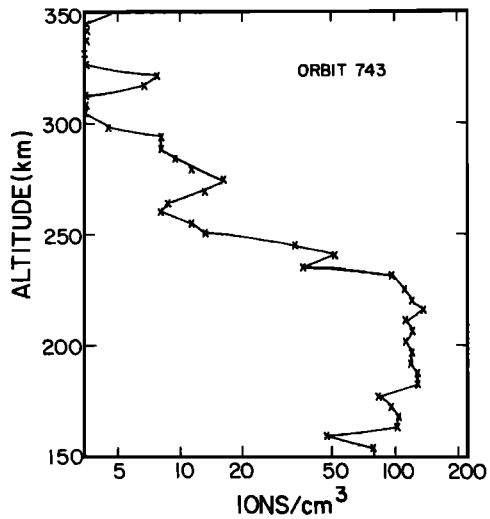

Fig. 10. Mg^+ density profile for orbit 743. The parameters of the observation are listed in Table 3.

a strong spatial gradient in the ion density in the trajectory plane. Referring again to Figure 1, a given altitude is observed from various locations, and the distance between two extreme observations (A and D) exceeds 1000 km. Consequently, if longitudinal and/or local time gradients are present, each inverted spin will produce a different profile such as represented in Figure 13. Once again, this late afternoon high-altitude tail is observed at a fairly low dip latitude.

Dip latitude dependence. The last two profiles suggest the existence of a magnetic latitude dependence of the *F* region Mg^+ density in the afternoon hours. This feature has been examined statistically by using the upward looking data of the wide angle channel collected on 42 circular orbits. These observations cover the period from November 20, 1976, to December 27, 1977, during which time the altitude varied from 240 to 290 km. Figure 14 presents the results of this study: the vertical intensity is plotted versus dip latitude in both hemispheres. Each data point represents the intensity measured between 1400 and 1600 LT and averaged in bins of magnetic inclination. The solid line is the smoothed arithmetic average

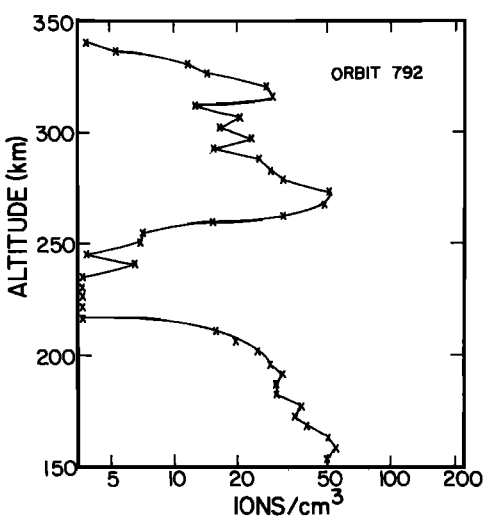

Fig. 11. Mg^+ density profile for orbit 792. The parameters of the observation are listed in Table 3.

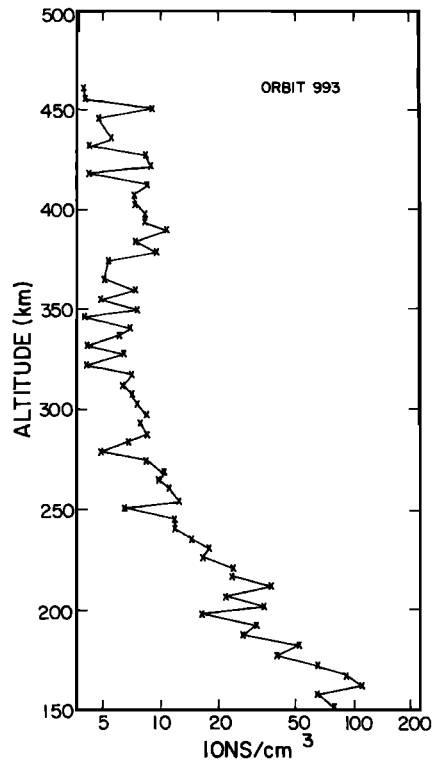

Fig. 12. Mg^+ density profile for orbit 993. The parameters of the observation are listed in Table 3.

of the observations. It is evident that the average intensity decreases with increasing magnetic inclination or dip latitude by almost an order of magnitude and that the variability of the *F* region column density is much higher near the dip equator (dip latitude $\lesssim 10°$) than at higher latitudes. These two con-

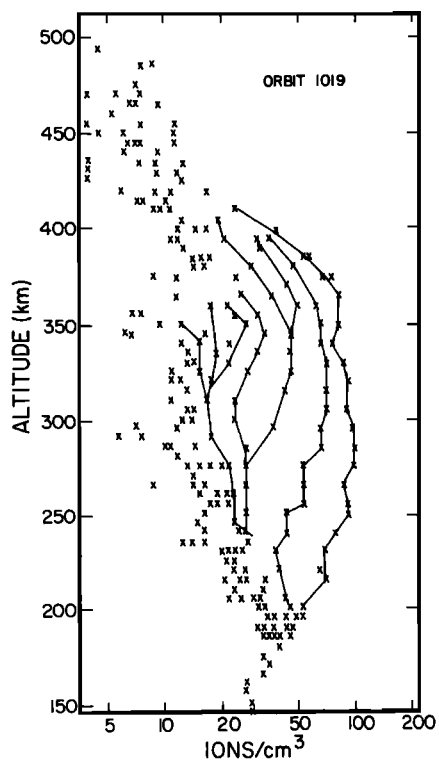

Fig. 13. Mg^+ density profile for orbit 1019. The parameters of the observation are listed in Table 3.

TABLE 3. Orbit Parameters for Data of Figures 9 to 13

Orbit	Date*	Local Time	Solar Zenith Angle, deg	Geographic Latitude, deg†	Geographic Longitude, deg‡	Dip Latitude, deg†
326	75350	8.0	72	17	−62	29
743	76018	13.5	25	−7	−52	3
792	76022	15.4	58	11	54	3
993	76038	17.5	85	7	−175	6
1019	76040	19.1	105	−6	−159	−5

*Read 75350 as day number 350 of 1975.
†Positive values refer to northern latitudes; negative values, to southern latitudes.
‡Positive values refer to east longitudes; negative values, to west longitudes.

clusions are in agreement with the results of the spinning inversions shown before: in the afternoon hours large densities of ions are usually only observed at very low latitudes, but even there the density may remain small at evening twilight. The fact that the southern hemisphere intensities tend to be weaker than the northern ones may reflect the fact that in the limited sample available the southern data were mostly collected in the Pacific sector. Hence it is not clear whether this is a latitude or a longitude effect. For the same reason, no seasonal information is available at this time, although it is expected that since seasonal effects are observed in the diurnal **E** × **B** drift variation, they probably also influence the density of metallic ions in the *F* region.

Discussion

The results of the morphological study of the magnesium ion distribution in the equatorial ionosphere made by the VAE experiment on AE-E may be summarized as follows:

1. A diurnal variation of the Mg^+ density is clearly observed. The maximum density occurs near 1400 LT and is located between 150 and 200 km.
2. The diurnal variations in the *E* region and the F_1 region are similar.
3. Mg^+ ions are present in the F_1 region as early as 1/2 hour after sunrise at all magnetic latitudes.
4. Ions are always observed in the F_1 region during daytime; there is no evidence of a latitude dependence. In contrast, the F_2 region is void of ions during morning hours. In the afternoon the distribution in the F_2 region depends strongly on dip latitude with larger densities always occurring near the dip equator.
5. Although variability is seen at every local time and place, it is most pronounced at very low latitudes during late afternoon.
6. There is evidence of the effect of winds and temporal variation of the **E** × **B** drift velocity.

Results 1, 4, 5, and 6 are consistent with the model developed by Hanson et al., which quantified the theory of *Martyn* [1959*a*, *b*]. Indeed, the fountain effect theory predicts that the metallic ion density will maximize in the F_2 region near the dip equator where the ions possess only a vertical velocity component and may reach higher altitudes than at other latitudes. The diurnal variation of the F_1 region reported here follows that of the vertical drift velocity measured at Jicamarca [*Woodman et al.*, 1977] during periods of solar maximum. It is not clear whether this is the behavior expected from the fountain effect; this point should be tested quantitatively by a model calculation. A possible explanation of the early afternoon peak would be the depletion of the metallic ion source by vertical transport. A calculation of the effect of vertical transport on the density is difficult, since chemical processes and motion along the field lines contribute to refill the depleted Mg^+ layer. There is observational evidence that there is no depletion, at least for the layer near 95 km. A mass spectrometer measurement by *Goldberg et al.* [1974] shows that the metallic layer is still present at evening twilight near the dip equator. Moreover, daytime measurements [*Aikin and Goldberg*, 1973] show no evidence of time variation of the density at low altitude.

Points 2 and 3 require some discussion. Obviously, the presence of ion densities exceeding 10 ions/cm³ at 150 km a few minutes after sunrise at dip latitudes as high as 30° does not appear to be consistent with the theory of the vertical polarization electric field raising ions from a source region at 95 km. In fact, as soon as the inclination of the magnetic field lines reaches a few degrees, this vertical velocity component of the drive decreases dramatically. This fact explains the confinement of the equatorial electrojet to a very narrow latitude region about the dip equator. For example, Figure 4 by *Hanson et al.* [1972] shows that the vertical ion velocity at 100 km drops from 15 m/s to 0 m/s from 0° to 8° of dip latitude. Consequently, it is not possible for this field to move the ions by about 50 km in a few minutes at latitudes exceeding 20°. Calculations of the production rate of meteor ions show

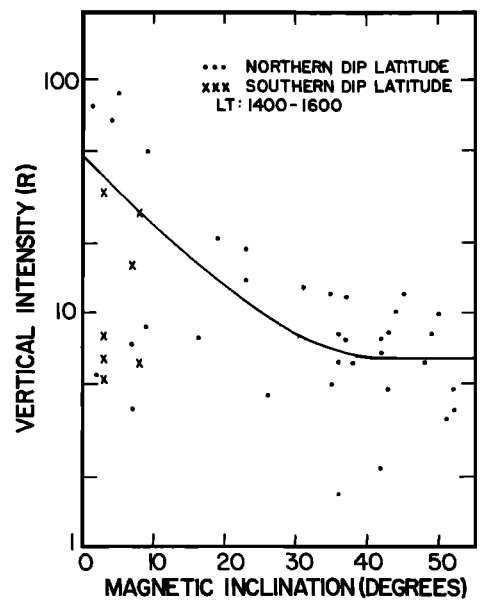

Fig. 14. Variation of the Mg^+ airglow intensity with magnetic inclination. The measurements were made between 14.00 and 16.00 hours local time from an altitude of approximately 260 km.

that evaporation of meteor atoms is the main source of meteor atoms below 120 km, whereas sputtering of micrometeorites becomes dominant above this altitude [*Lebedinets and Shushkova*, 1970]. This first component is strongly dependent on the meteor activity and is largely enhanced during meteor showers, but the second one is much more constant. This may explain why neither in these observations nor in earlier analysis was a correlation found with the meteor activity. Besides, mass spectrometer measurements of Mg^+ layers indicate that even at mid-latitude the distribution of ions extends well above 120 km in normal conditions [*Goldberg and Blumle*, 1970; *Narcisi*, 1972]. Very thin layers of metallic ions seem to be associated with the occurrence of sporadic E conditions [*Narcisi*, 1968; *Zbinden et al.*, 1975]. Consequently, there may be enough Mg^+ ions created or transported at 140 km by other means to allow the $\mathbf{E} \times \mathbf{B}$ drift to carry them into the F region without any need for a specifically equatorial mechanism in the lower E region. We, however, note the significance of dynamical processes as illustrated by the E region diurnal variation in the Mg^+ density.

We believe that the theory of the distribution of metallic ions at mid-latitude is not properly understood. Numerical modeling of the Mg^+ transport in the equatorial region should be able to test quantitatively if the fountain effect can reproduce the main features of the diurnal, latitudinal, and altitude distribution reported in this paper.

Acknowledgments. We gratefully acknowledge H. C. Brinton for providing us with Bims data. This work was supported in part by the National Aeronautics and Space Administration under grant NAS5-23006. One of the authors (J.C.G.) is supported by the Belgian Foundation for Scientific Research.

The Editor thanks R. A. Goldberg for his assistance in evaluating this paper.

REFERENCES

Aikin, A. C., and R. A. Goldberg, Metallic ions in the equatorial ionosphere, *J. Geophys. Res., 78,* 734, 1973.

Anderson, J. G., and C. A. Barth, Rocket investigation of the Mg I and Mg II dayglow, *J. Geophys. Res., 76,* 3723, 1971.

Brinton, H. C., L. R. Scott, M. W. Pharo III, and J. C. T. Coulson, The Benett ion-mass spectrometer on Atmosphere Explorer-C and -E, *Radio Sci., 8,* 323, 1973.

Gérard J.-C., Satellite measurements of high-altitude twilight Mg^+ emission, *J. Geophys. Res., 81,* 83, 1976.

Gérard, J.-C., and A. Monfils, Satellite observation of the equatorial Mg II dayglow intensity distribution, *J. Geophys. Res., 79,* 2544, 1974.

Gérard, J.-C., and A. Monfils, The Mg II equatorial airglow altitude distribution, *J. Geophys. Res., 83,* 4389, 1978.

Goldberg, R. A., and L. J. Blumle, Positive ion composition from a rocket-borne mass spectrometer, *J. Geophys. Res., 73,* 133, 1970.

Goldberg, R. A., A. C. Aikin, and B. V. Krishna Murthy, Ion composition and drift observations in the nighttime equatorial ionosphere, *J. Geophys. Res., 79,* 2473, 1974.

Grebowsky, J. M., and H. C. Brinton, Fe^+ ions in the high latitude F-region, *Geophys. Res. Lett., 5,* 791, 1978.

Hanson, W. B., and S. Sanatani, Meteoritic ions above the F_2 peak, *J. Geophys. Res., 74,* 3720, 1970.

Hanson, W. B., D. L. Sterling, and R. F. Woodman, Source and identification of heavy ions in the equatorial F layer, *J. Geophys. Res., 77,* 5530, 1972.

Hays, P. B., and R. G. Roble, A technique for recovering the vertical number density of atmospheric gases from planetary occultation, *Planet. Space Sci., 20,* 1727, 1972.

Hays, P. B., G. Carignan, B. C. Kennedy, G. G. Shepherd, and J. C. G. Walker, The visible-airglow experiment on Atmosphere Explorer, *Radio Sci., 8,* 369, 1973.

Lebedinets, V. N., and V. B. Shushkova, Meteor ionisation in the E-layer, *Planet. Space Sci., 18,* 1659, 1970.

Martyn, D. F., The normal F region of the ionosphere, *Proc. IEEE, 47,* 147, 1959*a*.

Martyn, D. F., Large-scale movements of ionization in the ionosphere, *J. Geophys. Res., 64,* 2178, 1959*b*.

Narcisi, R. S., Processes associated with metal-ion layers in the E-region of the ionosphere, *Space Res., VIII,* 360, 1968.

Narcisi, R. S., Mass spectrometer measurements in the ionosphere, in *Physics and Chemistry of Upper Atmospheres,* p. 171, D. Reidel, Hingham, Mass, 1972.

Wiese, W. L., M. W. Smith, and B. M. Glennon, Atomic transition probabilities, in *Hydrogen Through Neon,* vol. I, *NSRDS-NBS4,* National Bureau of Standards, Washington, D. C., 1966.

Wood, R. F., R. G. Rastogi, and C. Calderon, Solar cycle effects on the electric fields in the equatorial atmosphere, *J. Geophys. Res., 82,* 5257, 1977.

Zbinden, P. A., M. A. Hidalgo, P. Eberhardt, and J. Geiss, Mass spectrometer measurements of the positive ion composition in the D- and E- regions of the ionosphere, *Planet. Space Sci., 23,* 1621, 1975.

(Received January 4, 1979;
revised April 19, 1979;
accepted April 19, 1979.)